Manipulation of electric polarization with rotating magnetic field in a honeycomb antiferromagnet $Co_4Nb_2O_9$

N. D. Khanh,[1,2,*] N. Abe,[2] S. Kimura,[3] Y. Tokunaga,[2] and T. Arima[2]
[1]*Department of Physics, Tohoku University, Sendai 980-8578, Japan*
[2]*Department of Advanced Materials Science, University of Tokyo, Kashiwa 277-8561, Japan*
[3]*Institute for Materials Research, Tohoku University, Sendai 980-8577, Japan*
(Received 5 August 2016; revised manuscript received 31 July 2017; published 27 September 2017)

Honeycomb-based materials have been attracting a lot of attention owing to their fascinating physics as exemplified by the emergence of a massless Dirac fermion and a spin liquid state. We have investigated magnetoelectric (ME) phenomena in a honeycomb magnet $Co_4Nb_2O_9$ and observed a unique ME response associated with a simple antiferromagnetic ordering on the honeycomb network. The induced electric polarization changes its direction by an angle -2θ around the trigonal axis upon rotating the magnetic field by an angle θ. We attribute the variation of electric polarization direction in a rotating magnetic field to the continuous rotation of the magnetic moment on the honeycomb. Our findings may open a variety of novel ME responses based on a honeycomb magnet.

DOI: 10.1103/PhysRevB.96.094434

Two-dimensional honeycomb magnets have attracted a lot of attention due to their fascinating physics and possible application for future electronic devices. Although numerous intriguing phenomena related to honeycomb magnetic systems have been realized, there have been quite a few concerning the research about the magnetoelectric (ME) coupling in this class of materials. Up to the first order of the expansion of the free-energy function, the dependence of polarization (magnetization) on an external magnetic field (electric field) can be termed as the linear ME effect, which can be observed in the medium where both time-reversal and space inversion symmetries are broken simultaneously [1]. During the past several decades, the ME effect and related concepts, such as the toiroidal moment [2], the electromagnon [3], or the topological ME effects [4] have received much consideration due to their intriguing and abundant physics [5,6].

Among a number of honeycomb magnets that exhibit ME coupling, we select $Co_4Nb_2O_9$, which crystallizes in a centrosymmetric trigonal space-group $P\bar{3}c1$ (No. 165) [7] as a target material. Co^{2+} ions form a buckled honeycomb sheet within a trigonal basal plane which stacks along the trigonal axis as displayed in Fig. 1. The buckled honeycomb network accompanied with strong spin-orbit coupling of Co^{2+} ions makes this material a promising candidate to explore interesting phenomena inheriting the feature of honeycomb magnets as suggested in several recent theoretical works [8,9]. Note that, in addition to $Co_4Nb_2O_9$, the ME response of other materials that belong to the $A_4B_2O_9$ system (here A is divalent transition metals, and B represents Nb or Ta) also are being investigated intensively. The effect was discovered for the first time in the 1970s by Fischer and co-workers using powder samples [10]. Recently, the study of a magnetic property and ME coupling in $Mn_4Nb_2O_9$ were carried out by Cao *et al.* [11] and Fang *et al.* [12]. Polycrystals of $Co_4Ta_2O_9$, $Mn_4Ta_2O_9$, and Co_4NbTaO_9 also were found to exhibit the ME effect by Fang *et al.* [13], Liu *et al.* [14], and Liu *et al.* [15], respectively, which make $A_4B_2O_9$ compounds become rich platforms to examine the ME effect.

Fang *et al.* studied ME coupling in polycrystals of $Co_4Nb_2O_9$ and observed a large coupling constant of 18.4 ps/m [16]. Recently, in contrast with previous reports, we found that Co^{2+} magnetic moments are aligned antiferromagnetically in plane (magnetic space-group $C2/c'$ and propagation vector $\boldsymbol{k} = 0$) instead of pointing along the trigonal axis (magnetic space-group $P\bar{3}'c1$) [17]. Magnetic moments are nearly parallel to the $[1\bar{1}0]$ axis with a small canting along the [001] direction. Thus, a magnetic field applied along the $[1\bar{1}0]$ axis can cause a spin-flop phase transition at a critical magnetic-field $\mu_0 H_c \approx 0.2$ T, which aligns all magnetic moments normal to the field direction. Accordingly, a large polarization of 200 $\mu C/m^2$ was found along the [110] direction in a magnetic field of 7 T applied along the [110] or $[1\bar{1}0]$ axis, whereas a small one was observed along the trigonal axis [17]. More interestingly, the appearance of polarization parallel or perpendicular to a magnetic field suggests the formation of a magnetic monopole [18] or ferrotoroidic order [2] in the same system, respectively. Therefore, intriguing phenomena related to these novel concepts can be expected, such as ME birefringence [19,20] or directional dichroism [21,22]. Other recent works also report interesting aspects, which provide a wider understanding about the nature of the magnetic and ME properties of this compound [23–27].

However, there still remain some features that we do not clearly understand yet. An important issue is how the in-plane electric polarization evolves upon changing the magnetic-field direction. In order to clarify the relationship between the magnetic structure and the induced electric polarization, we carried out a measurement of the electric polarization of $Co_4Nb_2O_9$ in a rotating magnetic field within the trigonal basal plane up to 14 T. We found that the polarization is reversed not only by sweeping a magnetic field from positive to negative, but also under a 90° rotation of the external magnetic field within the trigonal basal plane. The phenomenon can be discussed based on the evolution of the magnetic structure on the honeycomb network in a rotating magnetic field. This effect should be distinguished from that of other typical linear

*Current address: RIKEN Center for Emergent Matter Science (CEMS), Wako, Saitama 351-0198, Japan.

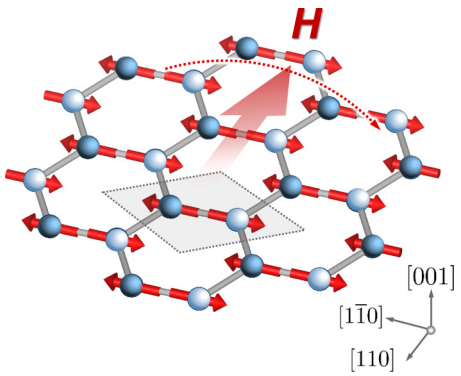

FIG. 1. Schematic Co^{2+}'s magnetic structure ordering in a honeycomb lattice upon a magnetic field rotating around the trigonal axis.

ME materials. Our finding may contribute to a new clue toward unveiling the microscopic origin of the ME effect in $Co_4Nb_2O_9$, which is still a mystery.

Single crystals of $Co_4Nb_2O_9$ were grown by a floating zone method [17]. The crystal structure was confirmed by powder x-ray diffraction. X-ray Laue photographs were used to determine the crystal axes. Samples were cut into thin rectangle plates for the measurement of magnetization and electric polarization. Magnetic properties were investigated by a superconducting quantum interference device (Magnetic Property Measurement System, Quantum Design). Electric polarization along different crystal axes was obtained via a measurement and subsequent integration of a displacement current with respect to time. To explore the effect of the magnetic-field direction on electric polarization, $Co_4Nb_2O_9$ samples were rotated around the trigonal axis in a magnetic field perpendicular to the rotation axis. Prior to the angle-dependence measurement, both the magnetic-field $\boldsymbol{H}$ and the poling electric-field $\boldsymbol{E}_P$ were applied at well above T_N. After the sample was cooled down to 5 K under the presence of both $\boldsymbol{H}$ and $\boldsymbol{E}_P$, only $\boldsymbol{E}_P$ was removed. Most of these experiments were carried out in a magnetic field up to 14 T by using a superconducting magnet installed at the High Field Laboratory for Superconducting Materials, Institute for Materials Research, Tohoku University, Japan.

Figure 2(a) presents electric polarization $P_{[110]}$ along the [110] axis as a function of magnetic-field direction θ when a magnetic field of 14 T rotates within the basal plane. The measurement was carried out at 5 K. Here one should note that the in-plane magnetic anisotropy of Co moments is weak and that a spin-flop transition is observed at around 0.2 T [Figs. 3(i) and 3(j)], which is much weaker than 14 T. The angle θ denotes the direction of magnetic-field $\boldsymbol{H}$ with respect to the [1$\bar{1}$0] axis. Thus, $\theta = 90^\circ$ when $\boldsymbol{H}$ is in the [110] direction, whereas $\theta = -90^\circ$ denotes the opposite direction of $\boldsymbol{H}$. Intriguingly, we observed a periodic variation of $P_{[110]}$ upon the rotation of $\boldsymbol{H}$ around the trigonal axis. After the ME poling in the $\boldsymbol{H} \perp \boldsymbol{E}_P$ configuration with $\boldsymbol{H} \| [1\bar{1}0]$ and $\boldsymbol{E}_P \| [110]$, $P_{[110]}$

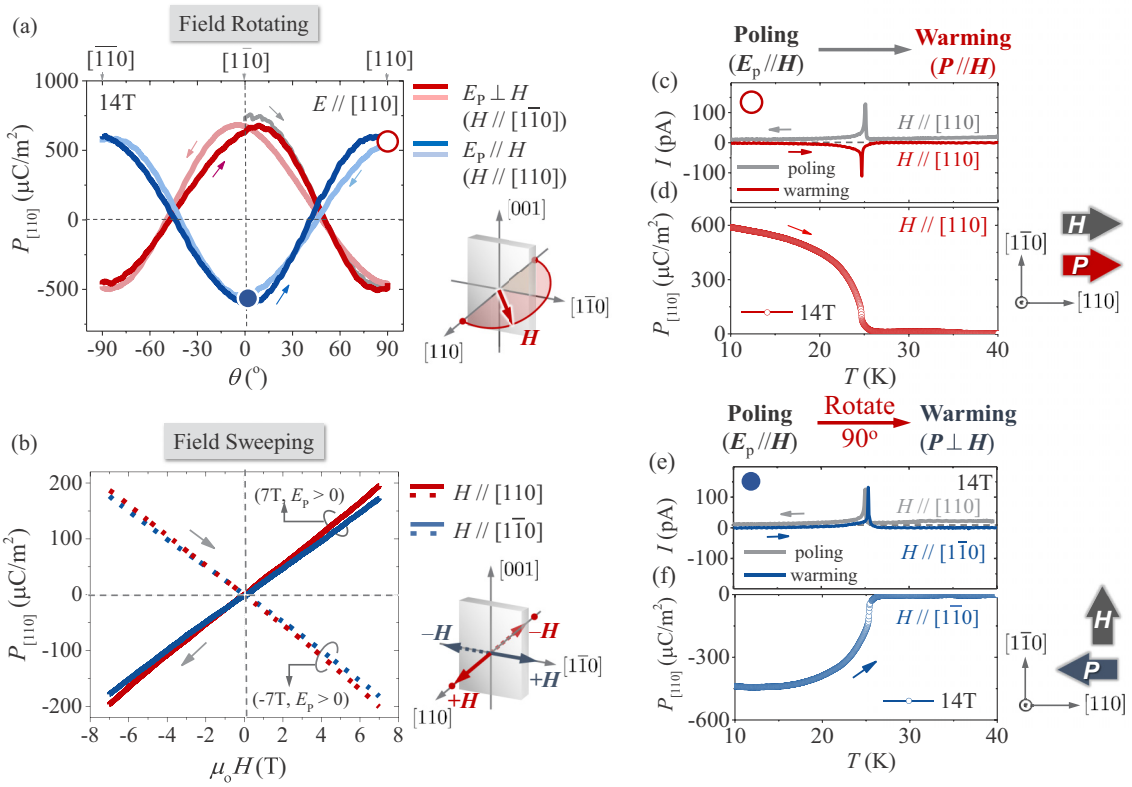

FIG. 2. (a) The dependence of $P_{[110]}$ on angle θ defined by the relative direction of magnetic-field $\boldsymbol{H}$ and the [1$\bar{1}$0] axis in $\mu_0 H = 14$ T and $T = 4.2$ K. θ is swept between $+90^\circ$ ($\boldsymbol{H} \| [110]$) and -90° ($\boldsymbol{H} \| [\bar{1}\bar{1}0]$). The open and solid circles mark the positions where temperature-dependent polarizations were measured in Fig. 3. To compare with the case of field sweeping, $P_{[110]}$ as a function of magnetic-fields $\boldsymbol{H} \| [110]$ and $\boldsymbol{H} \| [1\bar{1}0]$ was shown in (b).

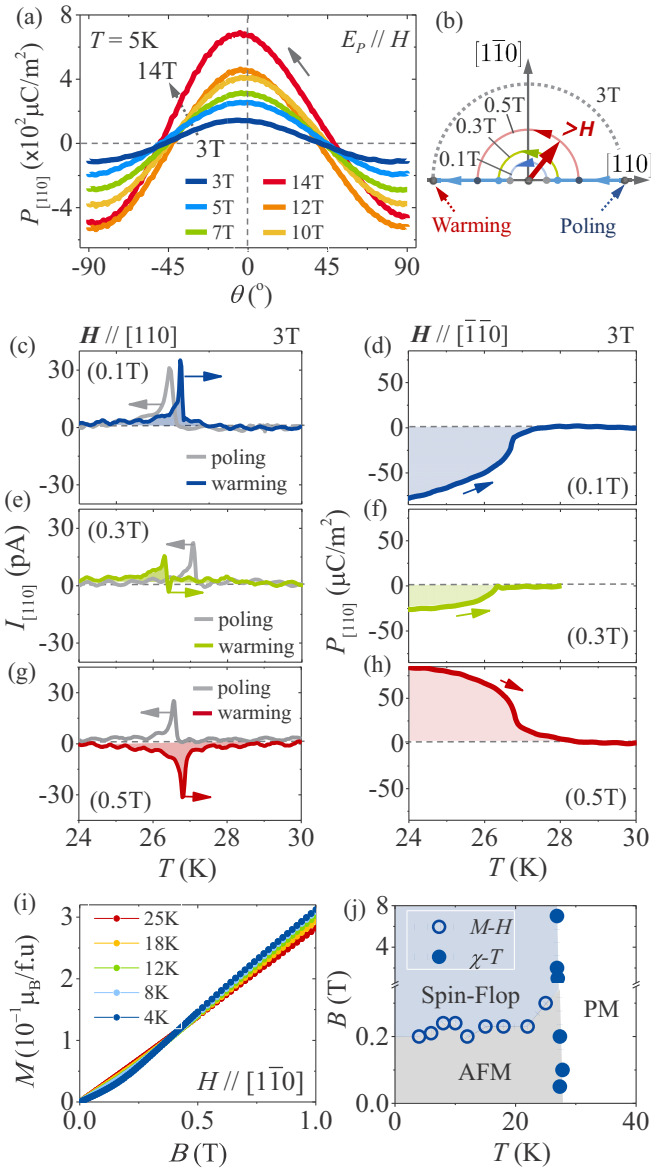

FIG. 3. (a) $P_{[110]}$ as a function magnetic-field direction θ at several magnetic fields from 14 T down to 3 T. (b) Schematic of an experimental procedure to measure the polarization in a rotating magnetic field of 0.1, 0.3, and 0.5 T. The displacement current and electric polarization along the [110] direction measured at 3 T after a rotating magnetic field at (c) and (d) 0.1 T, (e) and (f) 0.3 T, and (g) and (h) 0.5 T. (i) Temperature dependence of magnetization along the $[1\bar{1}0]$ direction. The data were summarized as a magnetic-field-temperature phase diagram for $\boldsymbol{H}\|[1\bar{1}0]$ in (j).

gradually decreases from $\sim 700\ \mu C/m^2$ at $\theta = 0$ and changes its sign from positive to negative at $\theta = 45°$, then reaches the minimum value of $\sim -600\ \mu C/m^2$ at $\theta = +90°$. This behavior was confirmed by a sweeping magnetic-field angle θ between $+90°$ and $-90°$, which clearly indicates a periodical change in $P_{[110]}$. This indicates that the polarization direction can be reversed by rotating the magnetic field by 90°, and a 180° rotation of the magnetic field results in a retention of the polarization. Finally, the periodical variation of polarization is also sensitive to the poling condition, i.e., whether $\boldsymbol{E}_P\|\boldsymbol{H}$ or $\boldsymbol{E}_P \perp \boldsymbol{H}$. As can be seen in Fig. 2(a), poling the sample in $\boldsymbol{E}_P\|\boldsymbol{H}\|[110]$ does not affect the periodic behavior of $P_{[110]}$ except that its sign was reversed.

For comparison, we show in Fig. 2(b) $P_{[110]}$ in a magnetic field sweeping along the [110] and $[1\bar{1}0]$ axes up to 7 T (here $P_{[110]}$ in $\boldsymbol{H}\|[110]$ was cited from Ref. [17]). In any case, a simple monotonic change in electric polarization in the magnetic field was observed as characterized by the linear ME effect. In principle, the rotation of the magnetic field between $+90°$ and $-90°$ is similar to the case of the sweeping magnetic field from $+\boldsymbol{H}$ to $-\boldsymbol{H}$ in the sense that the initial and final directions of $\boldsymbol{H}$ are opposite to each other. However, this observation suggests that $\boldsymbol{P}$ depends on $\boldsymbol{H}$ as an even function when $\boldsymbol{H}$ rotates around the [001] axis, whereas the conventional odd-function response of $\boldsymbol{P}$ to $\boldsymbol{H}$ was obtained by the sweeping magnetic field. This allows us to manipulate electric polarization in a distinct way by rotating the magnetic field.

This unique feature of the ME response can be confirmed by measuring $P_{[110]}$ as a function of temperature at $\theta = 90°$ and $\theta = 0°$, respectively [marked by open and closed circles in Fig. 2(a)] after poling in $\boldsymbol{E}_P \perp \boldsymbol{H}$ as shown in Figs. 2(c)–2(f). The displacement currents in poling and warming processes (with and without $\boldsymbol{E}_P$, respectively) were shown simultaneously with electric polarization $P_{[110]}$ obtained in a warming run after removing the electric field. As shown in Figs. 2(c) and 2(d), $P_{[110]}$ measured at $\boldsymbol{P}\|\boldsymbol{H}\|[110]$ is positive. Meanwhile, in the latter case, after poling in $\boldsymbol{E}_P\|\boldsymbol{H}\|[110]$, the magnetic field was rotated 90° from $\boldsymbol{H}\|[110]$ to $\boldsymbol{H}\|[1\bar{1}0]$ (corresponding to $\theta = 0°$). At this position, $P_{[110]}$ is negative, which clearly approves the reversal of the electric polarization rotation upon a 90° rotation of the magnetic field [Figs. 2(e) and 2(f)].

It should be mentioned that our observation should be distinguished with the reversal of polarization upon 90° rotating of the magnetic field in the typical linear ME system $Ni_3B_7O_{13}I$ [28]. In $Ni_3B_7O_{13}I$, when an in-plane magnetic field rotates 90° from [110] to $[1\bar{1}0]$, the out-of-plane polarization changes its direction 180° from [001] to $[00\bar{1}]$. Meanwhile, in $Co_4Nb_2O_9$, this relationship was established for all in-plane polarizations and magnetic fields. In addition, the ME effect was found in $Ni_3B_7O_{13}I$ in a weak ferromagnet phase whereas $Co_4Nb_2O_9$ exhibits an antiferromagnetic structure. As we will discuss below, the rotation of the polarization vector in $Co_4Nb_2O_9$ is constrained strongly with an antiferromagnetic structure. Most importantly, polarization in $Ni_3B_7O_{13}I$ depends on the magnetic field as an even function. This means that the effect of a rotating and sweeping magnetic field is similar in $Ni_3B_7O_{13}I$, which is quite distinct comparing to the scenario of $Co_4Nb_2O_9$.

The θ dependence of $P_{[110]}$ on the magnitudes of magnetic fields is displayed in Fig. 3(a). Decreasing the external magnetic field down to 3 T reduces the value of polarization $P_{[110]}$ without any effect on the qualitative behavior. One may raise the question how small a magnetic field one can use to switch the electric polarization. To answer this issue, the polarization $P_{[1\bar{1}0]}$ was measured as follows. A sample was first cooled in a magnetic field of 3 T and a positive electric field in a parallel configuration ($\boldsymbol{E}_P\|\boldsymbol{H}\|[110]$) down to 4.2 K. In this configuration, the polarization measured in the warming process should be positive. After removing the electric field, the magnetic field was decreased to 0.1, 0.3,

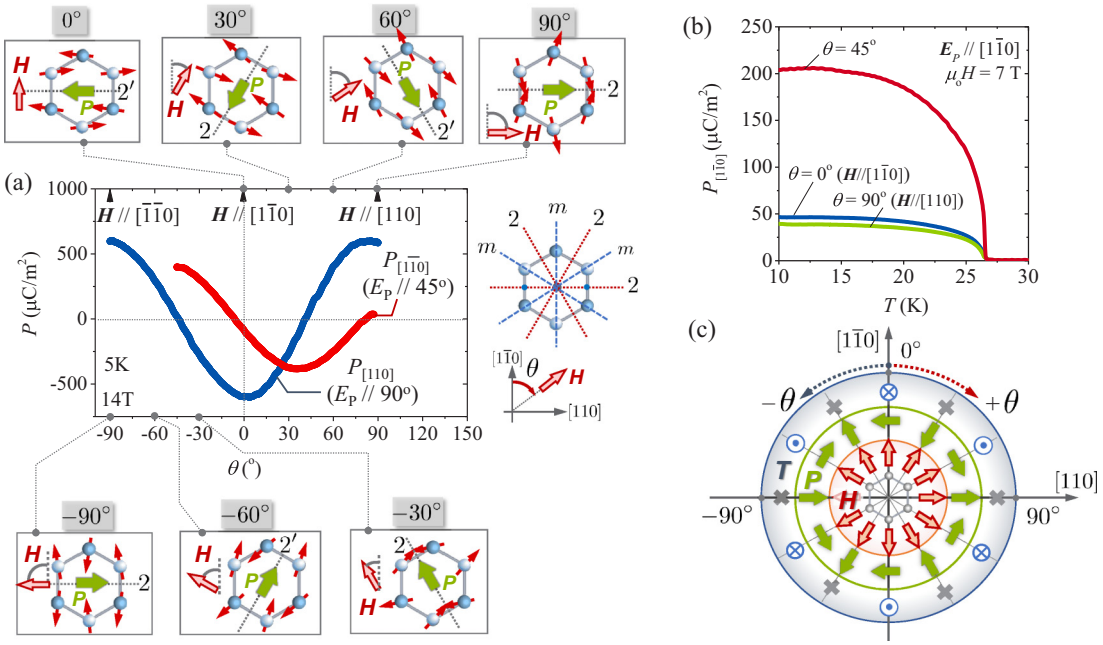

FIG. 4. (a) Periodical variation of $P_{[110]}$ poling at 0° and $P_{[1\bar{1}0]}$ poling at 45° under the rotation of the magnetic field. The correlation among the magnetic-field direction, the magnetic structure, the magnetic symmetry, and the induced polarization at each magnetic-field direction θ also is exhibited. (b) Comparison of the temperature dependence of $P_{[1\bar{1}0]}$ measured after poling in magnetic fields parallel to $\theta = 0°$, $\theta = 45°$, and $\theta = 90°$ ($\mu_0 H = 7$ T). (c) A summary of the relationship among the magnetic-field direction, the induced polarization, and the toroidal moment with respect to the in-plane rotation of the magnetic field, which clearly indicates that the polarization vector rotates an angle 2θ to the opposite direction upon changing the magnetic-field direction by an angle θ. The notation "×" denotes the absence of the toroidal moment $\boldsymbol{T}$ in $\boldsymbol{P} \parallel \boldsymbol{H}$ configurations.

or 0.5 T, followed by a rotation in the opposite direction before increasing again to 3 T as schematically illustrated in Fig. 3(b). Following this process, the temperature dependence of $P_{[110]}$ was measured at 3 T in a warming run. The results are illustrated in Figs. 3(c)–3(h). A conventional linear ME effect can be seen when the polarization changes its sign from positive to negative under the 180° rotation of the magnetic field of 0.1 T [Figs. 3(c) and 3(d)] and 0.3 T [Figs. 3(e) and 3(f)]. Meanwhile, a rotation of the magnetic field at 0.5 T results in the retention of polarization after changing the magnetic-field direction 180° as discussed above, which can be seen via positive temperature-dependent $P_{[110]}$ measured at 3 T [Figs. 3(g) and 3(h)]. Consider the fact that the polarization measured after rotating the magnetic field at 0.3 T is remarkably decreased and that a spin-flop phase transition occurs at around 0.2 T in $\boldsymbol{H} \| [1\bar{1}0]$ as shown in Figs. 3(i) and 3(j); we may conclude that such a kind of periodical variation of polarization can be obtained in the magnetic structure above the spin-flop transition field only. In brief, the significant features of the ME effect in $Co_4Nb_2O_9$ under rotating the magnetic field can be summarized as follows : the in-plane polarization was reversed upon rotating the magnetic-field direction by 90° and such a kind of phenomenon can be realized only in the spin-flop phase where magnetic moments all are aligned nearly perpendicular to the magnetic field.

According to the literature, the variation of electric polarization under the changing magnetic-field direction in the ME systems often closely relates to the modification of spin texture and magnetic anisotropy. For instance, in cases of spiral magnets $TbMnO_3$ [29] and $MnWO_4$ [30], the rotation of the magnetic field induces abrupt switching of the polarization due to a sudden flop of the spin spiral plane. Likewise, the flop of the polarization vector upon rotating the magnetic field was observed in helimagnets $CuFe_{1-x}Ga_xO_2$ [31], MnI_2 [32], and so on, originating from the variation of helical magnetic modulation vector $\boldsymbol{q}$. On the other hand, the continuous variation of the polarization vector with a field rotation has been found in several noncentrosymmetric magnets, such as $Ba_2CoGe_2O_7$ [33], Cu_2OSeO_3 [34], and CuB_2O_4 [35] where the polarization due to the spin-dependent metal-ligand hybridization mechanism emerges. Similarly, here we address the sinusoidal variation of $P_{[110]}$ in rotating $\boldsymbol{H}$ in $Co_4Nb_2O_9$ to the continuous rotation of every magnetic moment in the buckled honeycomb network. Consider $P_{[110]}$ measured after poling in $\boldsymbol{E}_P \perp \boldsymbol{H}$, and the vanishing of $P_{[110]}$ at $\theta = \pm 45°$ can be thought as a consequence of a 90° rotation of the polarization vector from initial position. In this sense, $P_{[1\bar{1}0]}$ should have the maximum value in a magnetic field applied along the $\theta = \pm 45°$ directions. To test this deduction, we measured $P_{[1\bar{1}0]}$ in a magnetic field at $\theta = \pm 45°$ and indeed observed the enhancement of electric polarization as shown in Fig. 4(a). The temperature dependence of $P_{[1\bar{1}0]}$ measured after poling in $\boldsymbol{H} \| [110]$ ($\theta = 90°$) or $\boldsymbol{H} \| [1\bar{1}0]$ ($\theta = 0°$) shows that the magnitude of $P_{[1\bar{1}0]}/H$ increased up to approximately four times larger when poling in $\theta = \pm 45°$ [Fig. 4(b)]. Due to the fact that the poling electric-field process can enhance the domain with polarization parallel to the poling electric-field direction, this result confirms that the polarization vector in fact changed its direction 90° from $\boldsymbol{P} \| [110]$ to $\boldsymbol{P} \| [1\bar{1}0]$ upon rotating the magnetic field 45°. Therefore, it can be seen that

similar to $P_{[110]}$, $P_{[1\bar{1}0]}$ exhibits a periodical modification upon magnetic-field rotation around the [001] axis, whereas the phase is shifted about 45° compared to that of $P_{[110]}$ [see Fig. 4(a)].

We next try to discuss the origin of the observed ME phenomena in a rotating magnetic field from the viewpoint of magnetic symmetry. First, when the measurement of polarization was carried out at a magnetic field above the spin-flop phase transition in $\boldsymbol{H}\|[1\bar{1}0]$, the ME response is related closely to the magnetic structure in the spin-flop phase rather than that of the zero-field ground state. Because the Co^{2+} moments have an easy-plane-type anisotropy as discussed above, the rotation of a high magnetic field around the [001] axis can rotate the Co^{2+} magnetic moments by almost the same angle and hence modify the electric polarization.

The unique ME response to a rotating magnetic field then relates to the buckled honeycomb network hosting three twofold axes and three vertical mirror planes. When a magnetic field is applied in the direction of $\theta = 0°$, the twofold symmetry along the [110] turns into $2'$ symmetry, and the other five symmetry operations are broken. As a result, depending on the poling condition, the polarization should orient in the [110] (90°) or $[\bar{1}\bar{1}0]$ (−90°) directions. Hereafter, let us assume that $P_{[110]}$ was negative. When the magnetic field is rotated from $\theta = 0°$ to $\theta = 30°$, all the Co^{2+} moments should be rotated clockwise by 30°. Then the twofold rotation around the $\theta = 30°$ axis revives, and accordingly, the polarization should be aligned parallel to this direction. This implies that the polarization vector rotated counterclockwise by 60° from the initial position of −90° to the direction of −150°. Further rotating the magnetic field to $\theta = 60°$ leads to the rotation of all the Co^{2+} moments by 60° clockwise from the initial direction. Then along the $\theta = 150°$ ([010] axis), the $2'$-axis revives. The polarization vector now turns into the +150° direction after a further −60° rotation. Comparing this state with the initial state, one may note that the sign of $\boldsymbol{P} \times \boldsymbol{M}$ is reversed, which can be ascribed to the antiferromagnetic phase shift between the state obtained by a 60° rotation of the magnetic field and that obtained just by a 60° rotation of the whole antiferromagnetic honeycomb. Briefly speaking, as the magnetic field rotates clockwise by an angle θ, the polarization rotates counterclockwise by an angle twice larger than -2θ. As a consequence, the toroidal moment $\boldsymbol{T}$, defined by the product $\boldsymbol{P} \times \boldsymbol{M}$, was reversed after each 60° rotation of the magnetic field. These results were summarized in Fig. 4(c), which illustrates the relationship among the magnetic-field direction, polarization, and the toroidal moment. Importantly, it should be noted that, from the above model, the rotation direction of the polarization vector must rotate twice in the opposite way with respect to the rotation of the magnetic field to satisfy the constraint of symmetry, which is quite consistent with our observation.

Although the microscopic origin of the induced polarization by the magnetic field in $Co_4Nb_2O_9$ still is unclear, this continuous change in polarization with respect to the variation of the magnetic-field angle can be attributed due to the modification of the electric dipole due to the rotation of the Co^{2+} magnetic moments network upon rotating the magnetic field rather than due to the variation of the ME tensor component originating from the discrete change in magnetic symmetry as similar

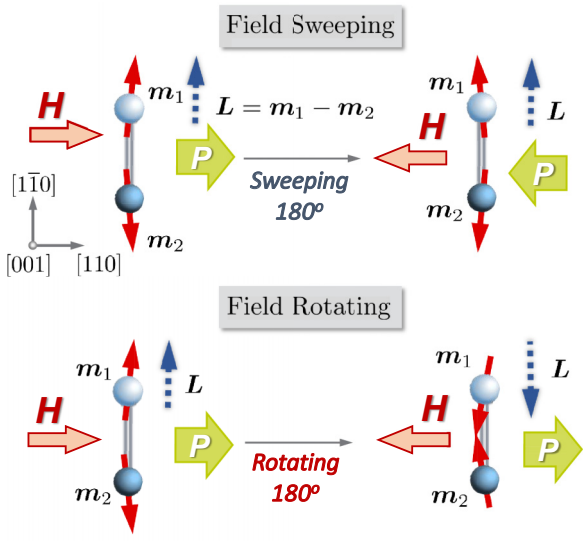

FIG. 5. (a) Periodical variation of $P_{[110]}$ poling at 0° and $P_{[1\bar{1}0]}$ poling at 45° under the rotation of the magnetic field. The correlation among the magnetic-field direction, the magnetic structure, the magnetic symmetry, and the induced polarization at each magnetic-field direction θ also is exhibited.

to the cases of CuB_2O_4, $Ba_2CoGe_2O_7$, or Cu_2OSeO_3. This result also is consistent with a recent theoretical study based on first-principles calculation [36], which plays an important role toward unveiling the microscopic mechanism of the ME response in this material.

As a consequence, the different behaviors of polarization upon rotating and sweeping the magnetic field can simply be understood as specific cases of $\theta = +90°$ and $\theta = -90°$, which schematically are demonstrated in Fig. 5. Here we conduct an explanation by considering neighboring Co^{2+} magnetic moments coupled antiferromagnetically to each other. In principle, the induced polarization in the linear ME effect in antiferromagnets under external magnetic-field $\boldsymbol{H}$ can be written in terms of $\boldsymbol{L} \cdot \boldsymbol{M} \propto \chi_M \boldsymbol{L} \cdot \boldsymbol{H}$, where $\boldsymbol{L} = \boldsymbol{m}_1 - \boldsymbol{m}_2$ is staggered, $\boldsymbol{M} = \boldsymbol{m}_1 + \boldsymbol{m}_2$ defines the uniform magnetization (here $\boldsymbol{m}_1$ and $\boldsymbol{m}_2$ are magnetic moments of the antiferromagnetic sublattice), and χ_M is the magnetic susceptibility. Under the sweeping magnetic field, $\boldsymbol{M}$ changes whereas $\boldsymbol{L}$ still is unchanged while external field $\boldsymbol{H}$ changes its sign, resulting in the reversal of $\boldsymbol{P}$. In contrast, upon rotating the magnetic field, both $\boldsymbol{M}$ and $\boldsymbol{L}$ change their signs, thus the signs of their products do not change, and retention of the polarization vector can be observed.

Finally, one also can discuss the effect of buckling based on these results as explained in Fig. 6. This can be evaluated through the comparison of the difference in the ME characteristics between the rotating antiferromagnetic moments only and the rotating whole honeycomb lattice. Note that the 60° rotation of the honeycomb affects the sign of buckling. If the ME response would be proportional to the magnitude of buckling, the 60° rotation of the whole antiferromagnet buckled honeycomb should maintain the sign of the ME tensor and $\boldsymbol{P} \times \boldsymbol{M}$, which resembles the process represented in Figs. 6(a)–6(c). However, we do observe the reversal $\boldsymbol{P} \times \boldsymbol{M}$ vector, which corresponds to the rotation

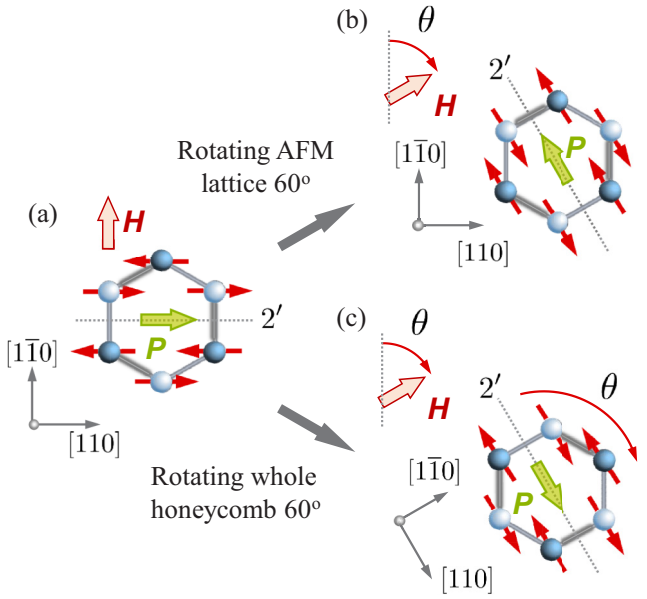

FIG. 6. Illustration the effect of buckling to the switching of polarization upon rotating magnetic field as can be examined via (b) rotating the magnetic structure only and (c) rotating the whole antiferromagnetic honeycomb layer from the initial position (a).

of the antiferromagnetic moments by [Fig. 6(b)] from the initial position [Fig. 6(a)]. Hence, it can be concluded that the buckling may not be crucial for the unique behavior of the ME response in this compound, i.e., -2θ rotation of $\boldsymbol{P}$ upon a θ rotation of $\boldsymbol{H}$.

To summarize, we have investigated the ME response in single-crystalline $Co_4Nb_2O_9$ in a rotating magnetic field within a trigonal basal plane. We found that the in-plane polarization also exhibited a periodical retention under a rotation of the magnetic field around the trigonal axis in the spin-flop phase. Changing the in-plane magnetic field by an angle θ causes the polarization vector rotating by an angle 2θ to the counterdirection. This effect can be attributed to the continuous rotation of the network of antiferromagnetic moments on the honeycomb lattice under the variation of the magnetic field. This feature is quite interesting among ME materials showing an odd response upon sweeping the magnetic field, which allows us to manipulate electric polarization by an external magnetic field in a distinct way. The unique feature of the ME response observed in this paper can be common in honeycomb antiferromagnets. It also should be noted that turning the magnetic-field direction is not the only way to switch the polarization vector [37]. Recently, uniaxial pressure has been proved as an effective tool to manipulate electric polarization in ME and multiferroic materials [38,39]. We expect such interesting phenomena may also occur in $Co_4Nb_2O_9$ by application of uniaxial pressure in sufficient directions, which would be exciting for future study.

We acknowledge H. Sagayama, Y. Nii, and K. Matsuura for stimulating discussions and N. Netsu for assistance with the experiments. This work was supported partly by Grants-In-Aid for Scientific Research (Grant No. 24244045) from the Japan Society for the Promotion of Science. The investigation of the ME response was carried out at the High Field Laboratory for Superconducting Materials, Institute for Materials Research, Tohoku University, Japan. The magnetic property and the x-ray Laue photograph were measured at the Institute for Solid State Physics, the University of Tokyo, Japan.

[1] M. Fiebig, J. Phys. D: Appl. Phys. **38**, R123 (2005).
[2] N. A. Spaldin, M. Fiebig, and M. Mostovoy, J. Phys.: Condens. Matter **20**, 434203 (2008).
[3] Y. Tokura and N. Kida, Philos. Trans. R. Soc., A **369**, 3679 (2011).
[4] A. M. Essin, J. E. Moore, and D. Vanderbilt, Phys. Rev. Lett. **102**, 146805 (2009).
[5] T. Arima, J. Phys. Soc. Jpn. **80**, 052001 (2011).
[6] Y. Tokura, S. Seki, and N. Nagaosa, Rep. Prog. Phys. **77**, 076501 (2014).
[7] E. F. Bertaut, L. Corliss, F. Forrat, R. Aleonard, and R. Pauthenet, J. Phys. Chem. Solids **21**, 234 (1961).
[8] S. Hayami, H. Kusunose, and Y. Motome, Phys. Rev. B **90**, 024432(R) (2014).
[9] S. Hayami, H. Kusunose, and Y. Motome, Phys. Rev. B **90**, 081115(R) (2014).
[10] E. Fischer, G. Gorodetsky, and R. M. Hornreich, Solid State Commun. **10**, 1127 (1972).
[11] Y. Cao, M. Xiang, Z. Feng, B. Kang, J. Zhang, N. Guiblin, W. Ren, B. Dkhil, and S. Cao, RSC Adv. **7**, 13846 (2017).
[12] Y. Fang, W. P. Zhou, S. M. Yan, R. Bai, Z. H. Qian, Q. Y. Xu, D. H. Wang, and Y. W. Du, J. Appl. Phys. **117**, 17B712 (2015).
[13] Y. Fang, S. Yan, L. Zhang, Z. Han, B. Qian, D. Wang, and Y. Du, J. Am. Ceram. Soc. **98**, 2005 (2015).
[14] B. B. Liu, Y. Fang, Z. D. Hana, S. M. Yan, W. P. Zhou, B. Qian, D. H. Wang, and Y. W. Du, Mater. Lett. **164**, 425 (2015).
[15] Y. Y. Liu, Y. P. Lu, L. Zhang, Y. Fang, Z. D. Han, B. Qian, X. F. Jiang, L. Y. Zhu, D. H. Wang, and Y. W. Du, RSC Adv. **6**, 95038 (2016).
[16] Y. Fang, Y. Q. Song, W. P. Zhou, R. Zhao, R. J. Tang, H. Yang, L. Y. Lv, S. G. Yang, D. H. Wangand, and Y. W. Du, Sci. Rep. **4**, 3860 (2014).
[17] N. D. Khanh, N. Abe, H. Sagayama, A. Nakao, T. Hanashima, R. Kiyanagi, Y. Tokunaga, and T. Arima, Phys. Rev. B **93**, 075117 (2016).
[18] N. A. Spaldin, M. Fechner, E. Bousquet, A. Balatsky, and L. Nordström, Phys. Rev. B **88**, 094429 (2013).
[19] T. Kurumaji, Y. Takahashi, J. Fujioka, R. Masuda, H. Shishikura, S. Ishiwata, and Y. Tokura, Phys. Rev. Lett. **119**, 077206 (2017).
[20] T. Roth and G. L. J. A. Rikken, Phys. Rev. Lett. **88**, 063001 (2002).
[21] T. Arima, J. Phys.: Condens. Matter **20**, 434211 (2008).
[22] S. Toyoda, N. Abe, S. Kimura, Y. H. Matsuda, T. Nomura, A. Ikeda, S. Takeyama, and T. Arima, Phys. Rev. Lett. **115**, 267207 (2015).
[23] Y. P. Lu, C. X. Ji, Y. L. Sun, Y. Fang, L. Zhang, Z. D. Han, B. Qian, X. F. Jiang, and W. P. Zhou, J. Alloys Compd. **679**, 213 (2016).

[24] Y. M. Xie, C. S. Lin, H. Zhang, and W. D. Cheng, AIP Adv. **6**, 045006 (2016).
[25] C. Dhanasekhar, S. K. Mishra, R. Rawat, A. K. Das, and A. Venimadhav, J. Alloys Compd. **726**, 148 (2017).
[26] I. V. Solovyev and T. V. Kolodiazhnyi, Phys. Rev. B **94**, 094427 (2016).
[27] G. Deng, Y. Cao, W. Ren, S. Cao, A. J. Studer, N. Gauthier, M. Kenzelmann, G. Davidson, K. C. Rule, J. S. Gardner, P. Imperia, C. Ulrich, and G. J. McIntyre, arXiv:1705.04017.
[28] E. Ascher, H. Rieder, H. Schmid, and H. Stossel, J. Appl. Phys. **37**, 1404 (1966).
[29] N. Abe, K. Taniguchi, S. Ohtani, T. Takenobu, Y. Iwasa, and T. Arima, Phys. Rev. Lett. **99**, 227206 (2007).
[30] K. Taniguchi, N. Abe, S. Ohtani, and T. Arima, Phys. Rev. Lett. **102**, 147201 (2009).
[31] S. Seki, H. Murakawa, Y. Onose, and Y. Tokura, Phys. Rev. Lett. **103**, 237601 (2009).
[32] T. Kurumaji, S. Seki, S. Ishiwata, H. Murakawa, Y. Tokunaga, Y. Kaneko, and Y. Tokura, Phys. Rev. Lett. **106**, 167206 (2011).
[33] H. Murakawa, Y. Onose, S. Miyahara, N. Furukawa, and Y. Tokura, Phys. Rev. Lett. **105**, 137202 (2010).
[34] S. Seki, S. Ishiwata, and Y. Tokura, Phys. Rev. B **86**, 060403(R) (2012).
[35] N. D. Khanh, N. Abe, K. Kubo, M. Akaki, M. Tokunaga, T. Sasaki, and T. Arima, Phys. Rev. B **87**, 184416 (2013).
[36] Y. Yanagi, S. Hayami, and H. Kusunose, *Japan Physical Society Annual Meeting, 71st Annual Meeting, Osaka University, 2017* (Japan Physical Society, Tokyo, 2017), p. 20aL22-4.
[37] H. Schmid, Proc. SPIE **4097**, 12 (2000).
[38] T. Nakajima, Y. Tokunaga, V. Kocsis, Y. Taguchi, Y. Tokura, and T.-h. Arima, Phys. Rev. Lett. **114**, 067201 (2015).
[39] T. Nakajima, Y. Tokunaga, Y. Taguchi, Y. Tokura, and T.-h. Arima, Phys. Rev. Lett. **115**, 197205 (2015).